Journal of Faculty of Engineering & Technology

journal homepage: www.pu.edu.pk/journals/index.php/jfet/index

# Facile Synthesis of CuS/Activated Kaolinite Composite for Photo-Fenton Degradation of Textile Dyes

F. Majeed[a], S. Rehmat*[a, b], M. Hassan*[a], M. M. Baig*[a], H. A. Ahmed[a], A. Razzaq[a], and M. U. Arif[c]

[a]Department of Chemistry, University of Narowal, Narowal, Pakistan

[b]Department of Chemistry, Government College University Lahore, Lahore, Pakistan

[c]ZJU-UIUC Institute, Zhejiang University, China

## Abstract

In this study, we successfully synthesized a CuS/activated kaolinite composite using a cost-effective co-precipitation method. In FTIR analysis, the appearance of vibration bands at 1107, 1017, and 803 $cm^{-1}$ confirmed the presence of $SO_4^{2-}$, Si-O, and Al (IV) functional groups in the composite. UV-visible spectroscopy demonstrated that the synthesized composite exhibited high degradation efficiency, achieving 98.1% degradation of cationic dye (crystal violet) and 90.2% degradation of anionic dye (methyl orange) within one hour through a Photo-Fenton reaction. The kinetic study revealed that the rate of degradation followed pseudo-first order ($R^2 > 0,95$) and the prepared catalyst could degrade 0.030 ppm and 0.01 ppm of crystal violet and methyl orange in one minute, respectively. Given its outstanding activity, the catalyst can be used for treating textile wastewater on the commercial level, especially when dealing with various types of dyes.

**Keywords:** Water pollution, Dyes, Fenton-like degradation, Composite

## 1. Introduction

Various activities like heavy industrialization, massive production of waste by humans, and careless utilization of natural resources are affecting the ecosystem, particularly water. Because of these activities, the unavailability of clean water has become the global challenge of the 21st century and now is the focal point of the research field. Diseases like cholera, skin irritation, intestinal tract infection, kidney failure, and cancer are reported due to the consumption of uncleaned water [1-3]. Among various categories of water pollutants, dyes are the most prevalent type of pollutant [4, 5]. Despite their vast applications in multiple industries, the huge production of synthetic dyes generates excess amounts of colored wastewater. They are referred to as recalcitrant pollutants because of their complex aromatic structure which makes them chemically stable, highly soluble in water, and not biodegrade easily, so they remain in the environment for longer periods [6-9]. From many studies, it is confirmed that dyes pointedly reduce the growth and development rate of plants [10, 11]. In humans, the greatest health hazard posed by textile dyes is genotoxicity [12] which results in mutations and may cause cancer [13]. Fenton and Photo-Fenton reactions have gained much attention as advanced oxidation processes (AOPs) because they offer energy-saving advantages, low-cost operation, easy magnetic iron separation, and quick decomposition of organic compounds using free solar radiation [14-16]. However, there are two critical problems to the conventional homogeneous Fenton process: (1) the reaction is operational only at pH 2-3, and (2) the formation of iron sludge [17].

Two-dimensional (2D) transition metal sulfides can be offered as a sustainable alternative. They exhibit layered structures and excellent characteristics like light absorption in the visible region, narrow band gap as compared to metal oxides, and give heterogenous Fenton-like reaction. Nickel sulfide has been reported as a Fenton-like catalyst, but it is stable in a highly alkaline environment and only degrades cationic dyes [18, 19]. Sulfides of copper (CuS), being a non-toxic p-type semiconducting material, are known for their remarkable photocatalytic and Fenton-like nature. It shows stability across a wide pH range and is easily synthesized through the co-precipitation method [20, 21]. Raj and Jaiswal have testified CuS nanoparticles and reported the degradation of cationic and anionic dyes under the influence of visible light, achieving degradation of 94-100% [22]. However, the nanoparticles are vulnerable to agglomeration, and their assembling through weak attractive forces limits their catalytic properties [23, 24]. To counter this issue, particle coating with a capping agent is mostly ascribed which reduces the agglomeration via electrostatic repulsion and stearic hindrance [25].

Kaolinite, a natural clay, has been used as a substrate for the generation of nanoparticles [26, 27]. It has a layered structure with 1:1 aluminosilicate and consists of a central octahedral aluminum oxide ($AlO_6$) sheet and a tetrahedral silica ($SiO_4$) sheet and both are connected through hydrogen bonding (Figure 1).

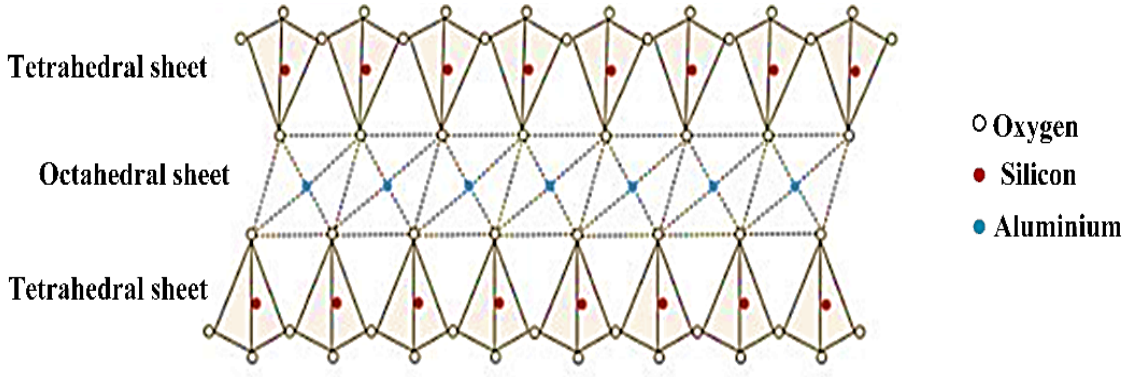


**Figure 1: Structure of kaolinite. Reprinted with permission from Ref. [28] Copyright 2023, Elsevier B.V.**

Naturally occurring kaolinite bears a small net negative charge due to the broken edges on the clay crystal. Moreover, a lot of work has been done to activate the surface of kaolinite including thermal and acidic treatment. The thermal treatment at a temperature of 400-900 $^oC$ results in the formation of a metakaolinite phase which is highly reactive [28, 29]. By subjecting kaolinite to acid activation, hydrolysis of Si-O-Al bonds occurred, leading to disruption of crystalline structure. This process results in the removal of octahedral $Al^{3+}$ ions and the formation of a more activated porous structure [30, 31].

Therefore, in this study, we used activated kaolinite as a capping agent to prepare a novel composite of CuS/Activated Kaolinite through co-precipitation for the Fenton-like degradation of dyes. This work has not been reported. This composite is developed and characterized to degrade both cationic dyes and anionic dyes which is another novel characteristic of this study.

## 2. Experimental

### *2.1. Chemicals*

Raw kaolinite, copper chloride dihydrate ($CuCl_2.2H_2O$, 99.95 %), thiourea ($H_2NCSNH_2$, 99 %), sulphuric acid ($H_2SO_4$, 95 %), ammonium hydroxide ($NH_4OH$, 97 %), crystal violet (97 %), methyl

orange (96 %). All chemicals are of analytical grade and were bought from Sigma Aldrich. The water was distilled in the laboratory for all experiments.

### *2.2. Surface activation of kaolinite*

The surface activation of kaolinite involved two steps [32]:

#### *2.2.1. Thermal treatment*

20 g of raw kaolinite was calcined at 650 °C in a muffle furnace over 3 h. The thermally treated clay is metakaolinite.

#### *2.2.2. Acidic treatment*

After thermal treatment, the clay was subjected to acid activation. Metakaolinite (10 g) was vigorously stirred in 100 ml $H_2SO_4$ solution (4mol $L^{-1}$) for 9 h. The activated clay was then washed with distilled water many times to achieve a neutral pH and dried for 5 h.

### *2.3. Preparation of copper sulfide/activated kaolinite composite*

The simple co-precipitation method was used to prepare pure CuS and its composite with activated kaolinite. Stock solutions of $CuCl_2.2H_2O$ and thiourea were prepared with the same molarities and volumes; 0.3 M in 300 ml water.

#### *2.3.1. Preparation of pure CuS*

Figure 2 presents the formation of pure CuS. 200 ml of Cu solution was taken in a container and stirred for 30 minutes. Subsequently, 200 ml of a thiourea solution was mixed with Cu solution upon stirring for another 30 minutes. The pH was maintained at 10 using $NH_4OH$. The mixture was again stirred for another 2 h with a temperature of 60-70 °C. Dark green precipitates were formed, the endpoint of the reaction. The resulting precipitates were subjected to multiple washes using water and were dried at 100 °C for 8 h [33].

#### *2.3.2. Synthesis of composite*

CuS/activated kaolinite composite was fabricated through co-precipitation as shown in Figure 3. Suspension of activated kaolinite (5.7 g) was created by stirring it in 70 ml of distilled water for 18 h. Next, 100 ml of 0.3 M Cu solution was introduced into the clay suspension and stirred for 3 h. After this period,100 ml of a thiourea solution was poured into the whole solution and again stirred for 24 h. The resulting precipitates were then thoroughly washed and dried at 100 °C for 10 h [24].

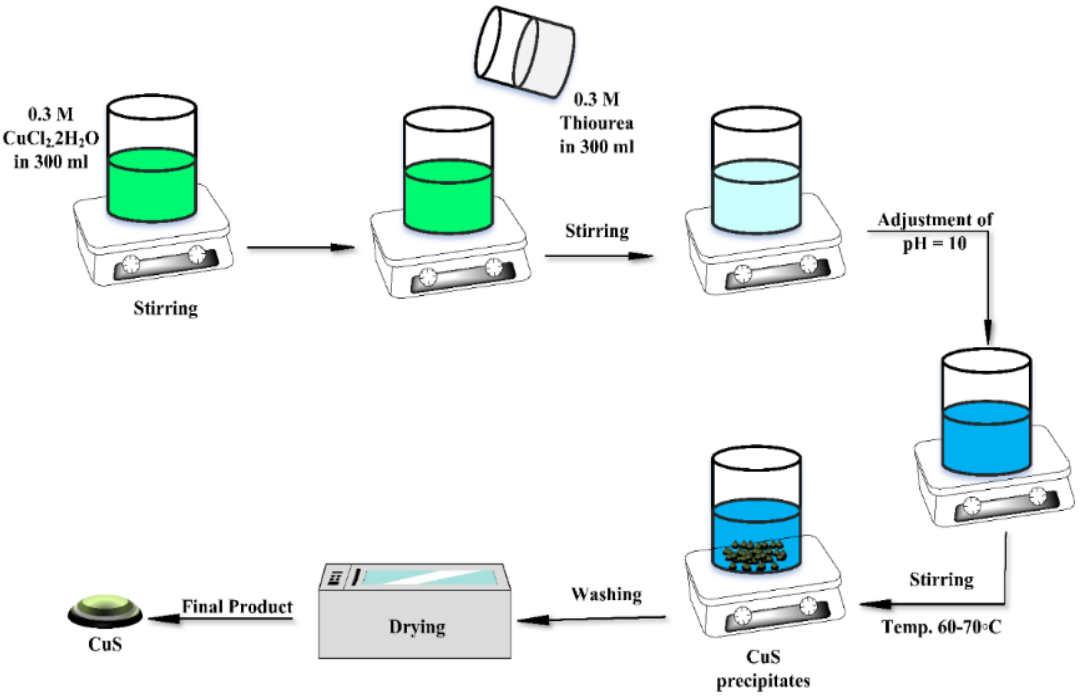


**Figure 2: Synthesis of pure CuS through co-precipitation method.**

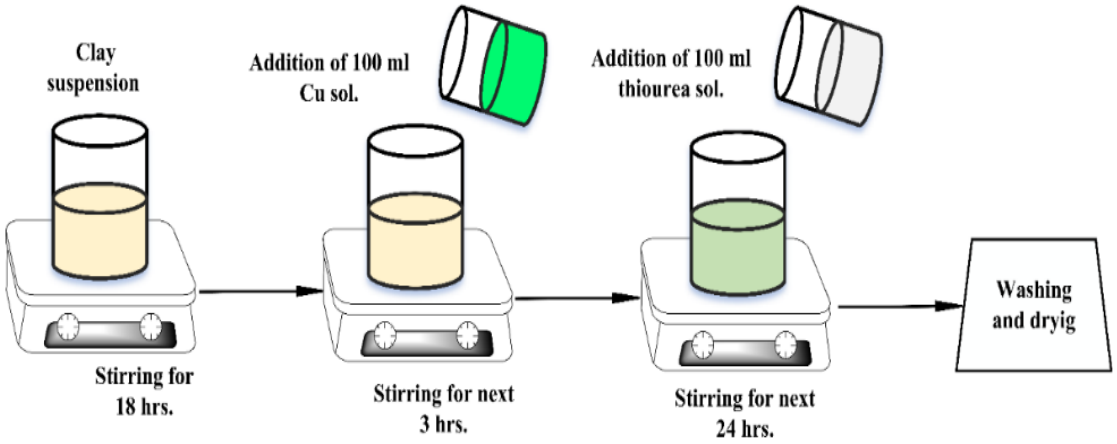


**Figure 3: Schematic synthesis of CuS/activated kaolinite composite through co-precipitation method.**

*2.4. Characterization and analysis*

*2.4.1. FTIR analysis*

The solid samples were desiccated under vacuum conditions and were individually positioned on Pike Miracle ATR cells to cover the surface of the ZnSe crystal. Subsequently, they were subjected to scanning within the spectral range of 4000 $cm^{-1}$ to 500 $cm^{-1}$. An average of 16 scans were acquired for each sample, maintaining a resolution of 2.0 $cm^{-1}$.

*2.4.2. Degradation experiments*

The CuS/activated kaolinite catalyst, as prepared, was employed in a Photo-Fenton reaction to degrade anionic (methyl orange (MO)) and cationic (crystal violet (CV)) dyes, both in the absence

and presence of visible light. In an experimental setup, 20 mg of the composite was introduced into 30 ml of dye solutions containing 10 ppm of the respective dyes. To these solutions, 1 ml of a 30 % $H_2O_2$ solution was added. For comparison, dye solutions of the same concentration were treated with 1 ml of 30 % $H_2O_2$ alone (without the catalyst) and pristine CuS/$H_2O_2$ (1 ml of 30 % $H_2O_2$). These mixtures were shaken for 30 minutes (maximum time) in the absence of light to attain adsorption-desorption equilibrium. After this dark period, the absorbance of the solutions was taken using a UV-visible spectrophotometer (model CECILE CE7200) at wavelengths of 585 nm (CV's $\lambda_{max}$) and 463 nm (MO's $\lambda_{max}$). The same procedure was repeated to assess dye degradation under visible light conditions, with irradiation provided by a 200 W Tungsten bulb.

The percentage degradation was measured using Eq (1):

$$\% \text{ Degradation} = \frac{C_0 - C_t}{C_0} \times 100 \quad (1)$$

Where, $C_0$ = Content of dyes at the time (0), and $C_t$ = concentration at time (t).

## 3. Results and Discussion

### *3.1. Structural analysis*

The FTIR spectrophotometer was used to examine the functional groups present in all samples within the 4000-500 $cm^{-1}$ range, using a Bruker Alpha-P FTIR Spectrophotometer. Figure 4 represents the transmittance peaks for all groups. The analysis of kaolinite revealed characteristic vibrations corresponding to the bonds in this clay mineral, including Al-O-H, Si-O, and Al-O. Specifically, the vibration at 3660 $cm^{-1}$ indicated the stretching of inner surface hydroxyl groups (OH) connected to the Al octahedral sheet. Another band at 1600 $cm^{-1}$ was observed across all samples, representing OH bending. After calcination at 650 °C, 3660 $cm^{-1}$ band disappeared, suggesting the dehydroxylation of raw clay and the formation of an amorphous intermediate structure known as metakaolinite. In addition, the frequency range of 1109-1000 $cm^{-1}$ in both raw and activated kaolinite samples was associated with Si-O stretching vibrational motion. The band at 949 $cm^{-1}$ was assigned to the stretching vibrational movements of Al-OH, while a new band at 803 $cm^{-1}$ indicated Al(IV)-O stretching vibrations, signifying the conversion of less active saturated Al atoms (Al(VI)) to more active unsaturated Al atoms (Al(V) and Al(IV))in the composite [29, 31, 32]. The band observed in the pristine CuS sample at 1107 $cm^{-1}$ can be ascribed to $SO_4^{2-}$ anti-symmetric stretch. It is clear from the graph that no peak corresponding to CuS ( IR inactive) was observed in FTIR [23]. The vibrations of Si-O and Al (IV)-O in the sample of CuS/Activated Kaolinite can be attributed to the successful formation of the composite.

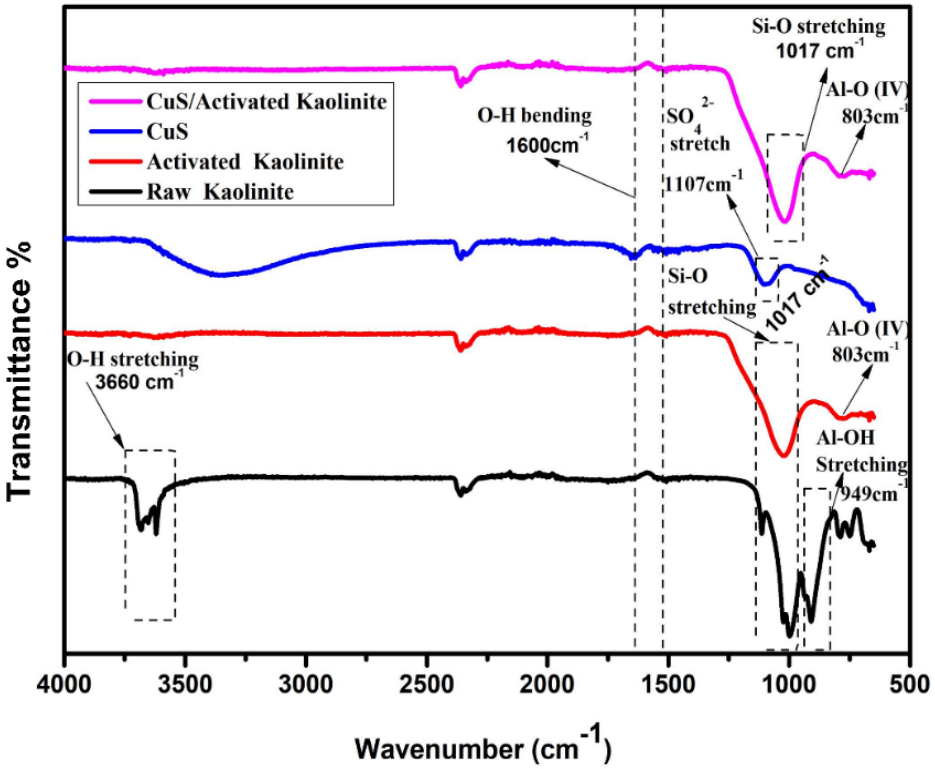


**Figure 4: FTIR spectra of raw kaolinite, activated kaolinite, CuS, and CuS/activated kaolinite composite.**

*3.2. Degradation analysis*

*3.2.1. Fenton-like catalytic degradation*

*1. Crystal violet*

The newly synthesized composite was tested for the removal of CV and the results are shown in Figure 5 (A) and (B). As given in Figure 5 (A), the intensity of the absorbance peak reduced with time, and after 1 h, the characteristic peak disappeared. First, the reaction was carried out in the dark for 30 minutes. The composite disclosed maximum degradation as compared to pristine CuS with percentages of 88.1 % and 70.8 %, respectively. The maximum elimination of dye by composite is also due to the inclusion of activated clay which provides a large surface area for the sorption of dyes. While $H_2O_2$ (control sample) only oxidized the dye up to 21 % in 30 minutes, showing the stability of the dye against $H_2O_2$. Next, all the readings were taken in visible light using a Tungsten bulb with an interval of 30 minutes. After 1 hour in light, the composite displayed a degradation percentage of 98.1 %, which proves that it is an efficient catalyst for the elimination of textile dyes. In comparison, the percentage of pristine CuS was 86.4 %. The clear difference between dye solutions before and after Fenton-like degradation is given in Figure 7.

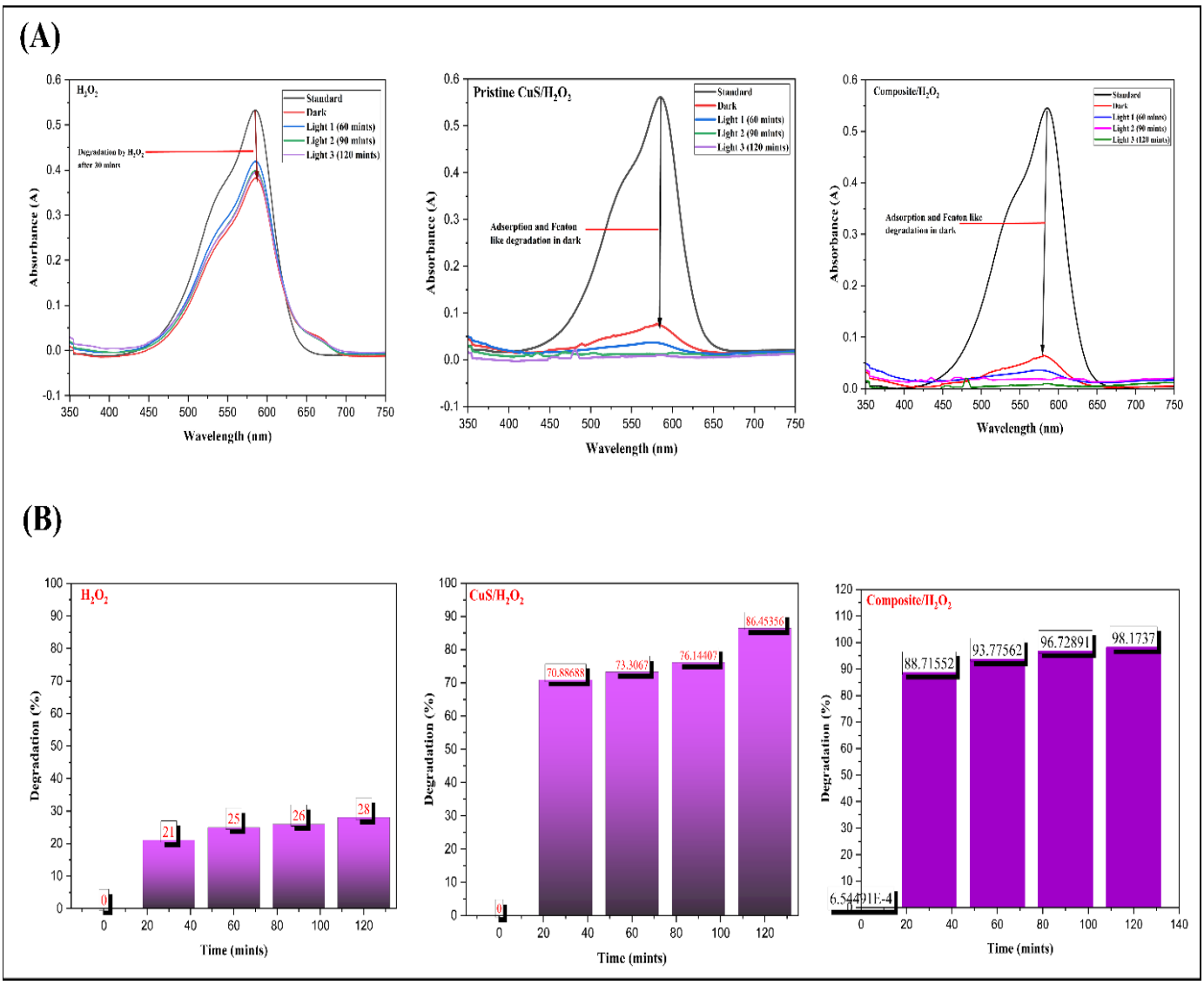


**Figure 5: Graphical representation of (A) degradation profile (B) percentage degradation of CV.**

*2. Methyl orange*

The same procedure was followed to check the degradation of MO. The UV-visible results (Figure 6) showed that the catalyst exhibits low degradation towards anionic dye as compared to CV under the dark, showing the selective nature of the catalyst. But still, it removed a maximum percentage of 40.9 % of dye as compared to pristine CuS (33.5 %). It should be noted that the Fenton-like degradation of MO was enhanced dramatically in the presence of visible light, from 40.2 % to 90.2 %. The enhancement in the degradation of MO demonstrates that this catalyst can be used for the deprivation of both anionic and cationic dyes.

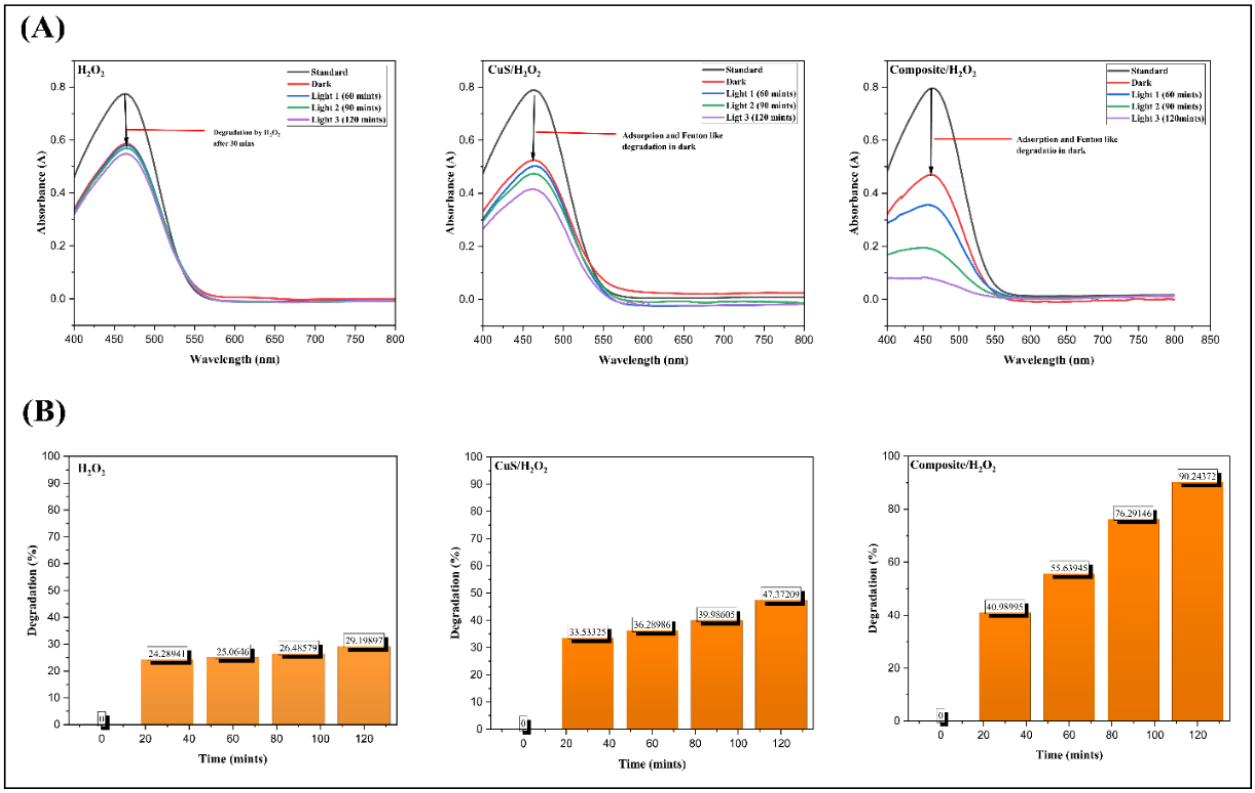


**Figure 6: Graphical representation of (A) degradation profile (B) percentage degradation of MO.**

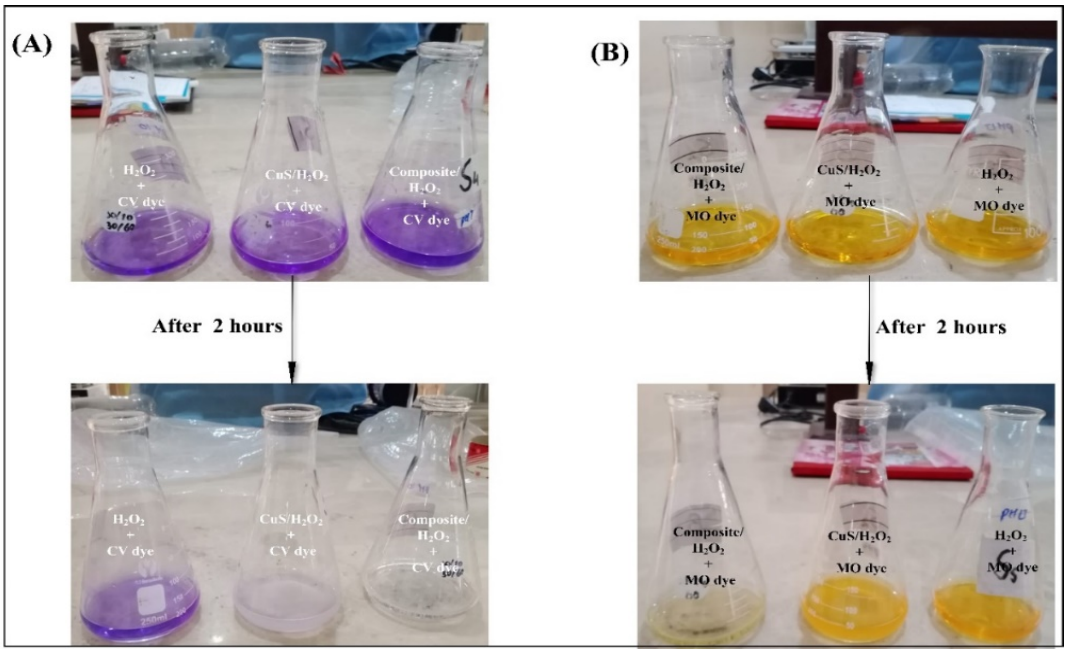


**Figure 7: (A) CV and (B) MO solutions before and after degradation.**

The degradation efficiency of CuS/Activated Kaolinite composite was investigated and compared with already published work in Table 1. The results revealed that our prepared composite showed maximum degradation efficiency against dyes (both cationic and anionic) within a short period in contrast to previously reported composites.

**Table 1. Comparison of present work with previous studies.**

| Sr. No. | Catalyst | Pollutants | Shaking Time (mints) | Catalyst Dose (mg $L^{-1}$) | % Degradation | Ref. |
|---|---|---|---|---|---|---|
| 1. | mont-La(6 %)-$Cu_{0.6}Cd_{0.4}S$ | phenol | 240 | 20 | 86 % | [34] |
| 2. | rGO-ZnS/CuS heterostructure | MO | 150 | 20 | 81.2 % | [35] |
| 3. | $FeNi_3/SiO_2/CuS$ magnetic nanocomposite | tetracycline | 90 | 50 | 96.71 % | [36] |
| 4. | CuS-ZnO nanocomposite | phenol and congo red | 120 | 20 | 82 % | [37] |
| 5. | CuS/Activated Kaolinite composite | CV<br>MO | 60 | 20 | 98.1 %<br>90.2 % | current work |

*3.3. Kinetic study of Photo-Fenton reaction*

The UV-visible data of catalytic degradation of CV and MO were used to investigate the kinetics and reaction rate. The analysis was conducted by applying the well-established Langmuir–Hinshelwood pseudo-first-order kinetic model. The apparent rate constant was subsequently determined through calculations based on rate Eq (2).

$$-\ln\frac{(C_t)}{(C_0)} = kt \qquad (2)$$

Where 'k' symbolizes the rate constant and talks about the order of reaction, while '$C_t$' and '$C_0$' stand for the dye concentration at a specific time 't', and at the start of the reaction, respectively. The observed pseudo-first-order rate constants ($R^2 > 0.95$) were derived from the slopes of the linear plots obtained when plotting $-\ln (C_t/C_0)$ against the irradiation time 't'. The results from UV-visible studies indicated that the coexistence of CuS/Activated Kaolinite composite and $H_2O_2$ enhances the degradation of the dye. In the case of CV, the rate constants of $H_2O_2$, $CuS/H_2O_2$, and composite/$H_2O_2$ were 0.001, 0.012, and 0.030 $min^{-1}$, respectively (Figure 8). For MO, degradation rate constants were 0.002, 0.004, and 0.01 $min^{-1}$ displayed by $H_2O_2$, $CuS/H_2O_2$, and composite/$H_2O_2$, respectively (Figure 9). This shows that the freshly prepared catalyst has a fast rate of degradation of both dyes, degrading 0.030 ppm of CV and 0.01 ppm of MO in one minute.

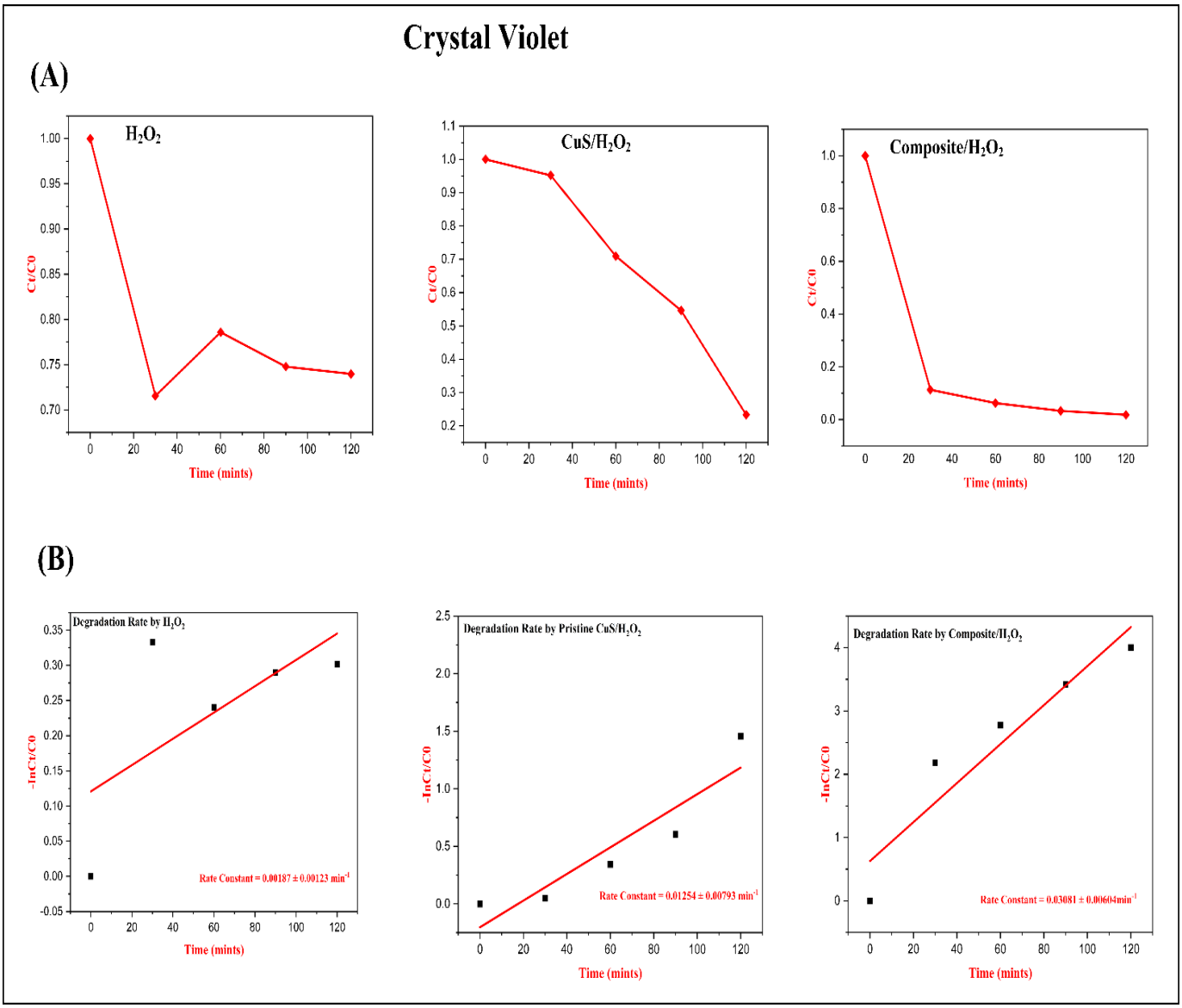


**Figure 8: Kinetic study of CV degradation.**

### *3.4. Mechanism of Photo-Fenton degradation*

Fenton-based chemical reactions entail the creation of reactive oxygen species (ROS). ROS are exceptionally potent oxidizing agents capable of reacting with organic compounds in a solution to fully oxidize them into carbon dioxide ($CO_2$) and water, a process known as organic mineralization [14, 38]. The reactive intermediates of this reaction involve hydroxyl radicals ($HO^{\cdot}$), reactive oxygen species—hydroperoxyl radicals ($HOO^{\cdot}$), superoxide radicals ($O_2^{\cdot-}$), and organic radicals (alkyl, peroxyl). When contaminates come in contact with these radicals, these radicals oxidize them to water and carbon dioxide [39, 40].

Under dark conditions, when $H_2O_2$ met CuS, hydroxyl radicals ($OH^{\cdot}$) were generated (Figure 10). Cu is in a +2-oxidation state as $Cu^{+2}$ in CuS. When CuS reacts with $H_2O_2$, it produces $Cu_{2-x}S$ through partial reduction of $Cu^{+2}$ ions and fractional break of disulfide and polysulfide bonds.

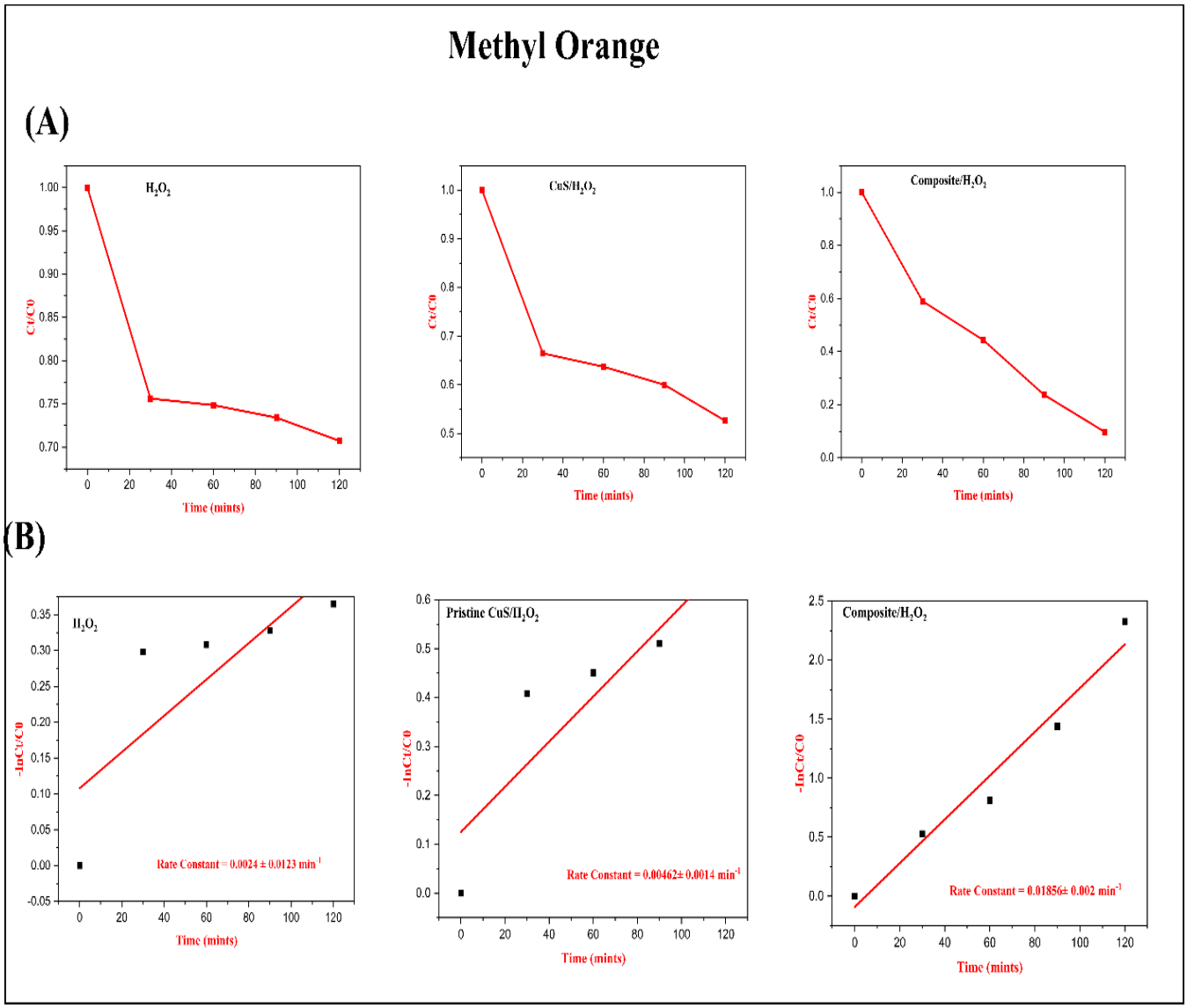


**Figure 9: Kinetic study of MO degradation.**

Moreover, sulfide ions in CuS can reduce $Cu^{+2}$ to $Cu^{+1}$. A reversible reaction of $Cu^{+2} \rightleftharpoons Cu^{+1}$ is started which continuously generates the $OH^{\cdot}$ radicals and degrades the organic dye. Additionally, the activated kaolinite clay provides a maximum surface area and active sites to adsorb the colored molecules. In visible light, the degradation rate reaction dramatically increased. This is because CuS also acts as a photocatalyst. When light falls on it, electrons from the valance band (VB) absorb photons of light and get excited. These excited electrons ($e^{-}$) reach in the conduction band (CB). As a result, holes ($h^{+}$) are created in the valance band, and electron-hole pairs are generated, which react with oxygen and water to generate highly reactive superoxide ($O_2^{-\cdot}$) and hydroxyl radicals, which in turn interact with dye molecules and ultimately fasten the rate of deprivation. In addition, $H_2O_2$ also acts as an electron acceptor. So, it takes in the photo-induced electrons from the conduction band and subsequently generates $OH^{\cdot}$ radicals and also inhibits the electron-hole recombination, and promotes the Photo-Fenton and photocatalysis process [22, 41]. So, the combination of adsorption, Fenton reaction, and photocatalysis provided by the composite, has overall enhanced the degradation of dyes.

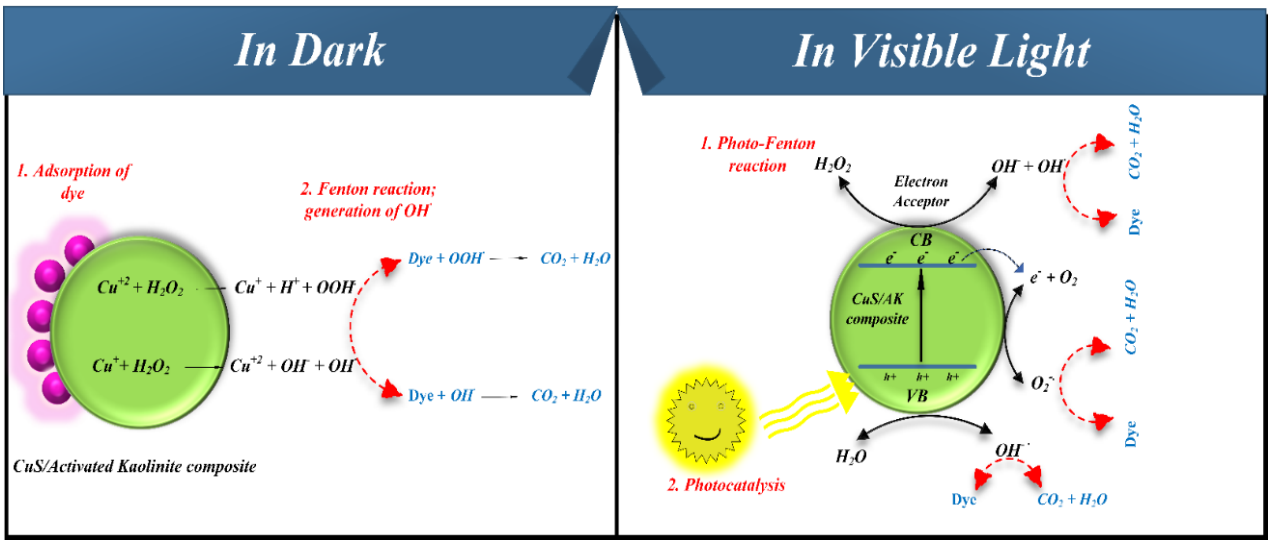


**Figure 10: Schematic mechanism of dye eradication.**

*3.4.1. Degradation pathway of CV*

Drawing from GC/MS and LC/MS analysis of intermediates in the Fenton/CV reaction given in [42], two potential pathways for the degradation of CV were proposed, named Route 1 and Route 2. These pathways correspond to two different sites where •OH radicals can attack the CV molecule. The primary oxidizing agent responsible for generating •OH radicals is the reaction between $Cu^{+2}$ and $H_2O_2$. Although less potent oxidizing agents like $HO_2$• and $H_2O_2$ may also play a role, the focus is on •OH radicals as the primary oxidant in these degradation pathways. In Route 1, CV undergoes N-de-methylation. This occurs when •OH radicals target the methyl group within compound B as shown in Figure 11A. The formation of hydroxymethylated intermediates is an intermediate step in this process, and these intermediates are further subjected to •OH radical attacks, ultimately resulting in the N-de-methylation of CV. This process persists until it terminates in the creation of fully N-de-methylated dye molecules referred to as F intermediate. In Route 2, •OH radicals initiate the process by targeting the conjugated ring structure, creating a carbon-centered radical. This radical is then subject to an attack by molecular oxygen, followed by the cleavage of a chromophore structure (Figure 11B). This breakdown leads to the formation of diverse aliphatic products before achieving complete mineralization.

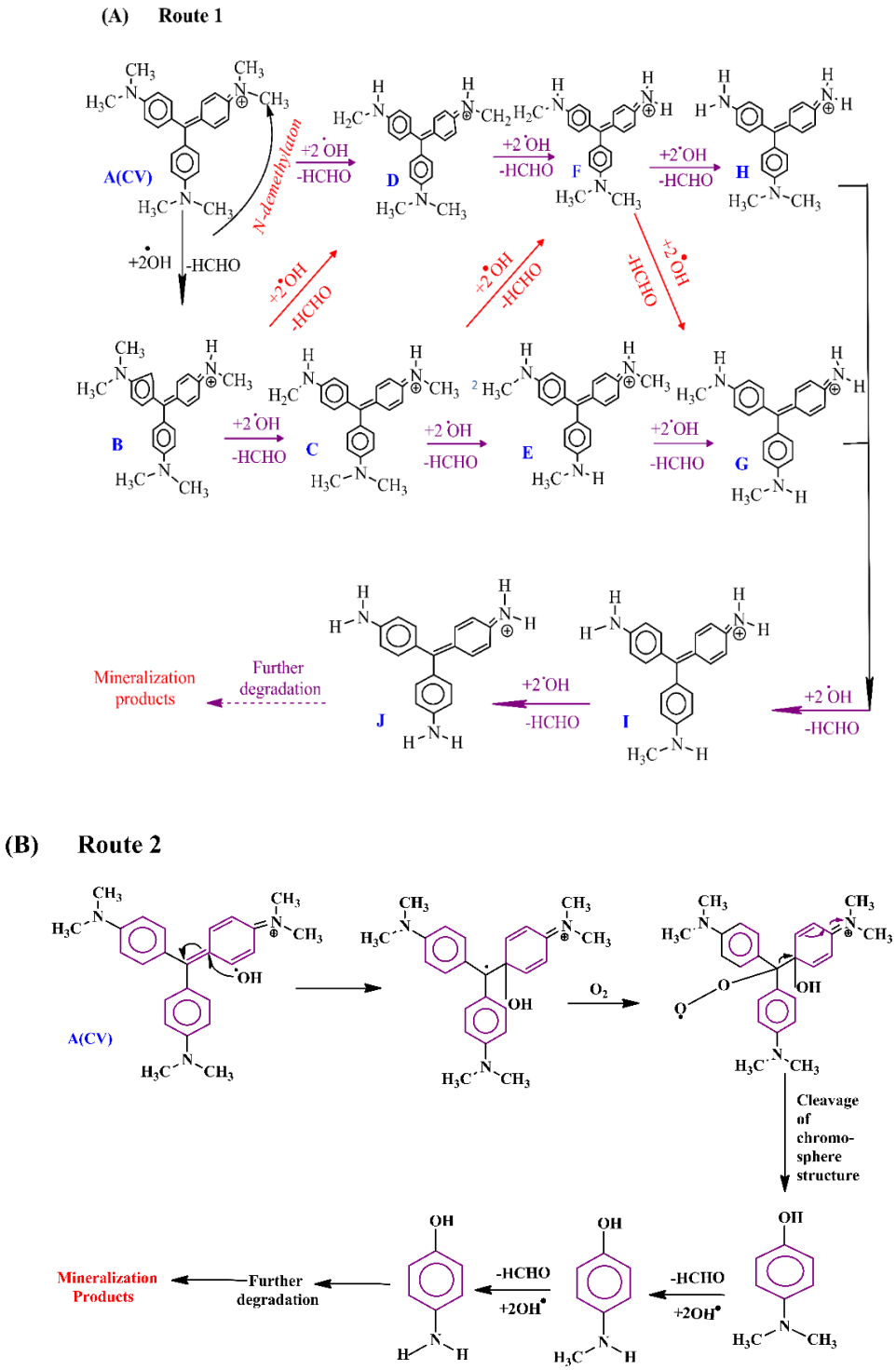


**Figure 11: Proposed degradation pathways of CV. Reprinted with permission from Ref. [42] Copyright 2009, Elsevier B.V.**

*3.4.2. Degradation pathway of MO*

MO degradation is a multi-step process. In the initial step, the conjugated structure of MO is disrupted. As indicated by the results of GC-MS analysis in references [43, 44], the degradation process involves the attack of hydroxyl radicals and subsequent breaking of the azo group (-

N=N-) that links the two aromatic rings, leading to the creation of aromatic amines with substituents (Figure 12). During the next stage, intermediates with structures resembling benzene rings trigger the disruption of the ring structure, leading to the creation of aliphatic chain compounds. These aliphatic chain compounds then undergo additional degradation processes, ultimately converting into carbon dioxide ($CO_2$) and water ($H_2O$) [45].

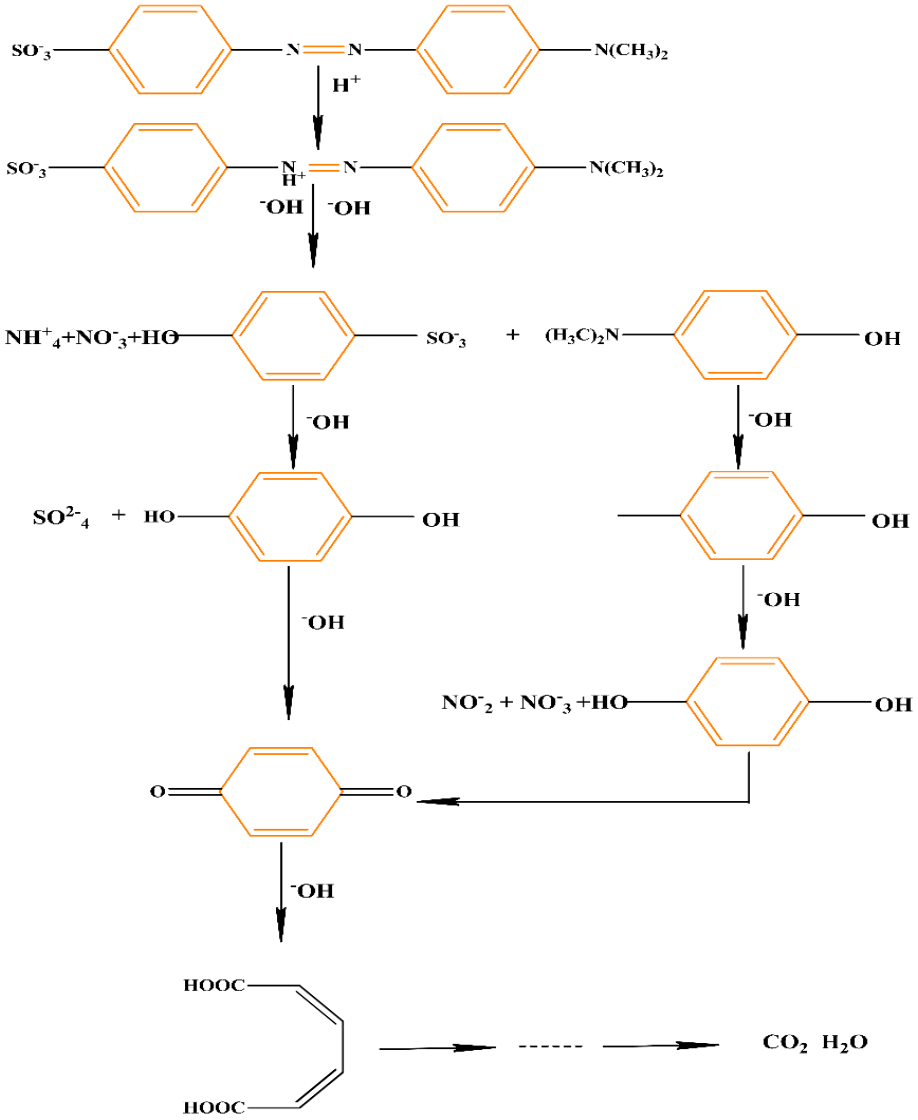


**Figure 12: Proposed degradation pathway of MO. Reprinted with permission from Ref. [43] Copyright 2016, Springer Nature.**

## 4. Conclusions

The composite of CuS/Activated Kaolinite was successfully synthesized by a cost-effective and eco-friendly method. The synthesized catalyst was used to check the degradation of CV and MO through the Photo-Fenton reaction. A comparative study was conducted between $H_2O_2$, pristine CuS/ $H_2O_2$, and composite/$H_2O_2$ for the removal of model dyes. Degradation results revealed that the newly synthesized catalyst has superior adsorption and removal efficiency with a percentage of 98.1% and 90.2% of CV and MO in 60 minutes, respectively, as compared to $H_2O_2$ (28%, 29%) and CuS/$H_2O_2$ (86.4%, 40.3%). Owing to the remarkable activity of the catalyst, this material can

be the best choice for textile wastewater treatment especially containing different types of dyes in the future.

**Acknowledgement**
The authors are thankful to the Department of Chemistry, University of Narowal for their contributions to this project.

**References**

[1]. S. Mehra, M. Singh, and P. Chadha, "Adverse impact of textile dyes on the aquatic environment as well as on human beings," *Toxicol Int,* 28 (2) (2021), 165.

[2]. A. R. Ribeiro et al., "An overview on the advanced oxidation processes applied for the treatment of water pollutants defined in the recently launched Directive 2013/39/EU," *Environ Int,* 75 (2015), 33-51.

[3]. C. K. Abdallah et al., *Advances in sustainable strategies for water pollution control: A systematic review* (IntechOpen, 2022), DOI: 10.5772/intechopen.108121.

[4]. S. Pai, M. S. Kini, and R. Selvaraj, "A review on adsorptive removal of dyes from wastewater by hydroxyapatite nanocomposites," *Environ Sci Pollut Res,* 28 (2021), 11835-11849.

[5]. S. Marimuthu et al., "Silver nanoparticles in dye effluent treatment: A review on synthesis, treatment methods, mechanisms, photocatalytic degradation, toxic effects and mitigation of toxicity," *J Photochem Photobiol B: Biol,* 205 (2020), 111823.

[6]. J. Sharma, S. Sharma, and V. Soni, "Classification and impact of synthetic textile dyes on Aquatic Flora: A review," *Reg Stud Mar Sci,* 45 (2021), 101802.

[7]. Y. Zhou et al., "Recent advances for dyes removal using novel adsorbents: a review," *Environ Pollut,* 252 (2019), 352-365.

[8]. R. D. Saini, "Textile organic dyes: polluting effects and elimination methods from textile waste water," *Int J Chem Eng Res,* 9 (1) (2017), 121-136.

[9]. M. Ahmaruzzaman and V. K. Gupta, "Rice husk and its ash as low-cost adsorbents in water and wastewater treatment," *Ind Eng Chem Res,* 50 (24) (2011), 13589-13613.

[10]. E. Rápó et al., "Performance comparison of Eichhornia crassipes and Salvinia natans on azo-dye (Eriochrome Black T) phytoremediation," *Crys,* 10 (7) (2020), 565.

[11]. S. Gita et al., "Toxicity evaluation of six textile dyes on growth, metabolism and elemental composition (C, H, N, S) of microalgae Spirulina platensis: the environmental consequences," *Bull Environ Contam Toxicol,* 106 (2021), 302-309.

[12]. B. Lellis et al., "Effects of textile dyes on health and the environment and bioremediation potential of living organisms," *Biotechnol Res Innov,* 3 (2) (2019), 275-290.

[13]. M. Shabbir and M. Naim, "Introduction to Textiles and the Environment," *Textiles and Clothing,* (2019), 1-9.

[14]. X. Liu et al., "Insight into electro-Fenton and photo-Fenton for the degradation of antibiotics: Mechanism study and research gaps," *Chem Eng J,* 347 (2018), 379-397.

[15]. M. Z. Asghar et al., "A new Y-Zr/g-C3N4 nanoflakes anchored mesoporous silica composite for efficient environmental remediation applications," *Diam Relat Mater,* 135 (2023), 109850.

[16]. M. M. Baig et al., "Green 2D simonkolleite/zinc based nanostructures for superior antimicrobial and photocatalytic applications," *Mater Chem Phys,* 287 (2022), 126292.

[17]. M. Fang et al., "CuO nanosheet as a recyclable Fenton-like catalyst prepared from simulated Cu (ii) waste effluents by alkaline H2O2 reaction," *Environ Sci: Nano,* 6 (1) (2019), 105-114.

[18]. A. Zhang, X. Huang, and Z. Nan, "Facile synthesis of 3D-structured NiS as an excellent Fenton-like catalyst under various pH through different mechanisms," *Inorg Chem,* 58 (20) (2019), 14136-14144.

[19]. M. Hassan et al., "Efficient water splitting catalyst: Low-temperature selenization of Co and Ni hydroxide nanosheets on carbon cloth for enhanced electro-catalytic activity," *Diam Relat Mater,* 139 (2023), 110298.

[20]. P. Roy and S. K. Srivastava, "Nanostructured copper sulfides: synthesis, properties and applications," *Cryst Eng Comm,* 17 (41) (2015), 7801-7815.

[21]. B. Pejjai, M. Reddivari, and T. R. R. Kotte, "Phase controllable synthesis of CuS nanoparticles by chemical co-precipitation method: effect of copper precursors on the properties of CuS," *Mater Chem Phys,* 239 (2020), 122030.

[22]. S. I. Raj and A. Jaiswal, "Nanoscale transformation in CuS Fenton-like catalyst for highly selective and enhanced dye degradation," *J Photochem Photobiol A: Chem,* 410 (2021), 113158.

[23]. S. Yadav and P. Bajpai, "Synthesis of copper sulfide nanoparticles: pH dependent phase stabilization," *Nano-Struct Nano-Objects,* 10 (2017), 151-158.

[24]. L. Zhang et al., "A facile preparation of montmorillonite-supported copper sulfide nanocomposites and their application in the detection of H2O2," *Sens Actuators B: Chem,* 239 (2017), 28-35.

[25]. Y. Zare, "Study of nanoparticles aggregation/agglomeration in polymer particulate nanocomposites by mechanical properties," *Compos A: Appl Sci Manuf,* 84 (2016), 158-164.

[26]. R. Xu et al., "Removal of heavy metal (loid) s from aqueous solution by biogenic FeS–kaolin composite: Behaviors and mechanisms," *Chemosphere,* 299 (2022), 134382.

[27]. Q. Li et al., "Removal of hexavalent chromium using biogenic mackinawite (FeS)-deposited kaolinite," *J Colloid Interface Sci,* 572 (2020), 236-245.

[28]. A. Hamza, I. A. Hussein, and M. Mahmoud, *Introduction to reservoir fluids and rock properties, in Developments in Petroleum Science* (Elsevier, 2023), 1-19.

[29]. M. Yu et al., "PbCl2 capture by kaolin and metakaolin under different influencing factors of thermal treatment," *Energy & Fuels,* 34 (2) (2020), 2284-2292.

[30]. H. Masihi and G. B. Gholikandi, "Using thermal-acidic-modified kaolin as a physical-chemical conditioner for waste activated sludge dewatering," *Chem Eng J,* 412 (2021), 128664.

[31]. J. Torres-Luna and J. Carriazo, "Porous aluminosilicic solids obtained by thermal-acid modification of a commercial kaolinite-type natural clay," *Solid State Sci,* 88 (2019), 29-35.

[32]. H. Cheng et al., "Enhanced PbCl2 adsorption capacity of modified kaolin in the furnace using a combined method of thermal pre-activation and acid impregnation," *Chem Eng J,* 414 (2021), 128672.

[33]. D. Pal et al., "Synthesis of randomly oriented self assembled CuS nanorods by co-precipitation route," *J Mater Sci: Mater Electron,* 30 (2019), 15700-15704.

[34]. H. Boukhatem et al., "Photocatalytic activity of mont-La (6%)-Cu0. 6Cd0. 4S catalyst for phenol degradation under near UV visible light irradiation," *Appl Catal B: Environ,* 211 (2017), 114-125.

[35]. B. Zeng et al., "Reduced graphene oxides loaded-ZnS/CuS heteronanostructures as high-activity visible-light-driven photocatalysts," *J Alloys Compd,* 582 (2014), 774-779.

[36]. N. Nasseh et al., "Synthesis and characterizations of a novel FeNi3/SiO2/CuS magnetic nanocomposite for photocatalytic degradation of tetracycline in simulated wastewater," *J Clean Prod,* 179 (2018), 42-54.

[37]. A. Q. Malik et al., "Synthesis, characterization, photocatalytic effect of CuS-ZnO nanocomposite on photodegradation of Congo red and phenol pollutant," *Inorg Chem Commun,* 143 (2022), 109797.

[38]. E. Brillas and S. Garcia-Segura, "Benchmarking recent advances and innovative technology approaches of Fenton, photo-Fenton, electro-Fenton, and related processes: A review on the relevance of phenol as model molecule," *Sep Purif Technol,* 237 (2020), 116337.

[39]. D. B. Miklos et al., "Evaluation of advanced oxidation processes for water and wastewater treatment–A critical review," *Water Res,* 139 (2018), 118-131.

[40]. A. V. Vorontsov, "Advancing Fenton and photo-Fenton water treatment through the catalyst design," *J Hazard Mater,* 372 (2019), 103-112.

[41]. W. Xu et al., "Nanoporous CuS with excellent photocatalytic property," *Sci Rep,* 5 (1) (2015), 18125.

[42]. H.-J. Fan et al., "Degradation pathways of crystal violet by Fenton and Fenton-like systems: condition optimization and intermediate separation and identification," *J Hazard Mater,* 171 (1-3) (2009), 1032-1044.

[43]. S. Xie et al., "A highly efficient degradation mechanism of methyl orange using Fe-based metallic glass powders," *Sci Rep,* 6 (1) (2016), 21947.

[44]. S. Filice et al., "Photo-Fenton Degradation of Methyl Orange with Dunino Halloysite as a Source of Iron," *Catalysts,* 12 (3) (2022), 257.

[45]. F. Wang et al., *Kinetics and possible mechanism of the degradation of methyl orange by microwave assisted with Fenton reagent* in *2011 5th International Conference on Bioinformatics and Biomedical Engineering*, 2011, IEEE.